Carbohydrate Polymers 84 (2011) 1117–1125

Contents lists available at ScienceDirect

Carbohydrate Polymers

journal homepage: www.elsevier.com/locate/carbpol

# Rheological properties of aqueous solution of new exopolysaccharide secreted by a deep-sea mesophilic bacterium

Hai-ping Li[a], Wan-guo Hou[a,b,*], Yu-zhong Zhang[c]

[a] Key Laboratory for Colloid and Interface Chemistry of Education Ministry, Shandong University, Jinan 250100, PR China
[b] Key Laboratory of Eco-chemical Engineering, Ministry of Education, College of Chemistry and Molecular Engineering, Qingdao University of Science and Technology, Qingdao 266042, PR China
[c] State Key Laboratory of Microbial Technology, Shandong University, Jinan 250100, PR China

ARTICLE INFO

*Article history:*
Received 18 August 2010
Received in revised form
29 November 2010
Accepted 24 December 2010
Available online 8 January 2011

*Keywords:*
Rheology
Oscillatory test
Thixotropy
Creep and recovery test
Critical concentration
SM-A87 EPS

ABSTRACT

The rheological properties, such as shear flow behavior, thixotropy and viscoelasticity, of aqueous solution of a new type of exopolysaccharide (SM-A87 EPS) secreted by a deep-sea mesophilic bacterium were investigated using shear flow and dynamic rheological measurements. For the SM-A87 EPS solutions, the overlapping concentration $C^*$ and crossover concentration $C^{**}$ were confirmed to be 0.95 g/L and 4.99 g/L respectively by the concentration-dependences of rheological parameters, such as equilibrium viscosity, thixotropic strength, static and dynamic stress, critical shear rate, and storage modulus in the linear viscoelastic region besides the zero-shear viscosity of solutions. At concentrations higher than $C^*$, the solutions exhibited a static stress, a dominant elastic behavior and a stronger absolute positive thixotropic strength. Otherwise, at concentrations lower than $C^*$, no static stress, a dominant viscous behavior and a weaker absolute positive thixotropic strength were exhibited. The SM-A87 EPS solutions may be used as enhanced oil recovery system.



## 1. Introduction

The family *Flavobacteriaceae*, belonging to the phylum *Bacteroidetes* [formerly *Cytophaga–Flavobacterium–Bacteroides*, (CFB)], includes a number of marine bacteria. Recently, a novel genus of the family *Flavobacteriaceae*, the mesophilic bacterium *Wangia profunda* SM-A87 (SM-A87), was isolated on marine agar 2216 medium (Difco) from deep-sea sediment samples taken from near the southern Okinawa Trough at a water depth of 1245 m using core sampler (Qin et al., 2007). In order to survive in the deep-sea nutrient-scarce environment, SM-A87 secretes large quantities of highly viscous exopolysaccharides (EPS) to concentrate proteinaceous particles and metal ions as a growth and energy source. The low-nutrient consuming and high yielding properties of the bacterium indicate that SM-A87 EPS might be a low-cost producer (Zhou, Wang, Shen, Hou, & Zhang, 2009). The SM-A87 EPS may be chemically considered as an anionic polyelectrolyte, expected to be used as food additives, sorbents (Zhou et al., 2009), emulsifier, stabilizer, thickener, enhanced oil recovery system and so on. Understanding the rheological behavior of SM-A87 EPS solution is of applied and fundamental importance.

Zero-shear viscosity, yield stress, thixotropy and viscoelasticity are the basic rheological properties which have received a lot of attention by many researchers (Barnes, 1999; Bradna, Quadrat, & Dupuis, 1995; Choi & Han, 2003; Chronakis & Alexandridis, 2001; Hou, Sun, Han, Zhang, & Wang, 1998; Lund, Lauten, Nyström, & Lindman, 2001; Moller, Mewis, & Bonn, 2006; Quadrat, 1985; Stadler et al., 2006; Takigawa, Kadoya, Miki, Yamamoto, & Masuda, 2006; Yang, Bick, Shandalov, Brenner, & Oron, 2009). Zero-shear viscosity ($\eta_0$) is the viscosity measured in shear deformation when the shear rate is approaching to zero (Biro, Gandhi, & Amirkhanian, 2009). Yield stress ($\sigma_0$) is another important rheological parameter for fluids. It is theoretically defined as the stress at which the fluid first starts moving when the applied stress increases or first stops moving when decreasing the applied stress (Barnes, 1999; Moller et al., 2006). The zero-shear viscosity and yield stress of polymer solutions could be determined by using many methods including equilibrium shear flow, creep and oscillatory shear (or sweep) measurements. The zero-shear viscosity and yield stress of polymer solutions were found to be different values depending on the measurement method and the experimental procedure (Barnes, 1999; Biro et al., 2009; Moller et al., 2006). It is possible that there is no way to measure the absolute values of them in the sense that they could be merely theoretical concepts (Barnes,

* Corresponding author at: Key Laboratory for Colloid and Interface Chemistry of Education Ministry, Shandong University, Jinan 250100, PR China.
Tel.: +86 0531 88364750; fax: +86 0531 88364750.
*E-mail address:* wghou@sdu.edu.cn (W.-g. Hou).

0144-8617/$ – see front matter © 2011 Elsevier Ltd. All rights reserved.
doi:10.1016/j.carbpol.2010.12.072

1999). However, the existence of problems cannot cover their great industrial applications, just as Nguyen and Boger (Barnes & Walters, 1985; Blair, 1933) put about yield stress: "Despite the controversial concept of the yield stress as a true material property. . ., there is generally acceptance of its practical usefulness in engineering design and operation of processes where handling and transport of industrial suspensions are involved." One method used for such applications is to work with two yield stresses, *i.e.*, static yield stress and dynamic yield stress (Moller et al., 2006; Papanagopoulos, Pierri, & Dondos, 1998). Static yield stress means the yield stress measured in an undisturbed sample while dynamic yield stress is the yield stress of a completely devastated sample, often determined from extrapolation of the equilibrium flow curve (Yang et al., 2009).

The thixotropy of fluids is a time-dependent rheological property. Hitherto, three types of thixotropy have been observed: "positive thixotropy", *i.e.*, time-dependent shear-thinning phenomenon of fluids such as drilling mud, paint, coating, etc.; "negative thixotropy", *i.e.*, time-dependent shear-thickening phenomenon of fluids mainly including polymer solutions (Bradna & Quadrat, 1984; Bradna et al., 1995; Quadrat, 1985); "complex thixotropy", *i.e.*, the phenomenon that a given fluid may show, early or late, positively thixotropic character and negatively thixotropic character, or vice versa (Hou et al., 1998). In general, three methods can be used to investigate the thixotropic properties of a fluid: monitoring the change of viscosity (or stress) with time at a given shear rate (Abu-Jdayil, Al-Malah, & Asoud, 2002), monitoring the recovery of viscosity (or stress) with time at a given low shear rate after intense shear (Hou et al., 1998; Li et al., 2003), and the hysteresis loop (Dolz, Bbugaj, Pellicer, Hernández, & Górecki, 1997). The so-called hysteresis loop is a diagram of shear stress as a function of shear rate, which is usually obtained through a three-step experiment. First, the shear rate is linearly increased with a given ramp from zero to a prefixed maximum value. This is followed by a keeping at the maximum shear rate for a given time (peak hold). Thereafter, the shear rate is reversely decreased at the same ramp from the maximum value to zero. During these steps the corresponding changes of shear stress *vs.* shear rate are automatically measured in a computer-based rheometer and up-curve and down-curve is obtained, respectively. It is well known that the hysteresis loop of up-curve above down-curve means positive thixotropy, and that of up-curve below down-curve means negative thixotropy, while the hysteresis loop with a crossover point means complex thixotropy (Dai, Hou, Duan, & Ni, 2007). The hysteresis loop area enclosed between up-curve and down-curve may be considered as an estimation of the degree of thixotropy. It is generally admitted that the greater the hysteresis area, the stronger the thixotropic property.

The concentration dependence of rheological properties of fluids is of critical importance for their industrial applications. Adam, Delsanti, and Jannink (1976) presented three concentration domains for polymer solution: dilute, semidilute, and concentrated solutions. The properties of polymer solutions tend to change rather abruptly in crossing over both from dilute to semidilute regimes and from semidilute to concentrated regimes (Adam et al., 1976). In dilute polymer solutions, the molecules are separated and the intrinsic properties of the individual molecule almost determine their physical properties. When the concentration increases gradually to a certain value $C^*$ (overlapping concentration), the molecules start to touch each other and entangle permanently. So $C^*$ is regarded as a critical concentration which separates the dilute and semidilute regimes. At higher concentrations, intermolecular entanglements strengthen and at another critical concentration ($C^{**}$), entangled polymer molecules gain a uniform polymer segment density. So $C^{**}$ is regarded as the boundary of semidilute and concentrated regimes (Roots & Nyström, 1979; Ying & Chu, 1987). In general, the first critical concentration $C^*$ and the second critical concentration $C^{**}$ of polymer solutions were determined by using the concentration dependence of zero-shear viscosity (Benchabane & Bekkour, 2008). Rodd, Dunstan, and Boger (2000) reported that dynamic light scattering method could be used to determine both the critical concentrations. It is also suggested that the second critical concentration could be considered as the critical concentration at which the viscoelastic properties do appear in polymer solutions according to dynamic (creep and frequency-sweep) measurement results (Benchabane & Bekkour, 2008; Ebagninin, Benchabane, & Bekkour, 2009).

In order to get a much refined insight into the rheological behavior of SM-A87 EPS solution, the zero-shear viscosity, yield stress, thixotropy and viscoelasticity of the solution were examined in this work, and the critical concentrations, $C^*$ and $C^{**}$, were determined based on the concentration dependence of these rheological properties. It was found that very similar values of $C^*$ and $C^{**}$ were obtained by using different measurement methods. The corresponding results may provide the basic information for its applications in enhanced oil recovery system.

## 2. Materials and methods

### 2.1. Materials

The dry sample of SM-A87 EPS was prepared with the method described in Ref. (Zhou et al., 2009). Fresh sample was stored in the refrigerator at 4 °C. The weight-average molecular weight was measured to be $3.76 \times 10^6$ g/mol with Gel Permeation Chromatographer (HP1100, Agilent) under the following conditions: column, 300 mm × 7.8 mm I.D. TSK-GEL G4000PWXL (10 μm particle size, 300 Å pore size, Tosoh Corporation, Minato-ku, Tokyo, Japan) with a TSK-guardcolumn; mobile phase, 0.1 M sodium chloride; flow rate, 0.5 mL/min; injection volume, 20 μL of 0.1% SM-A87 EPS solution; temperature, 25 °C (Fig. S1 in supporting information).

### 2.2. Methods

#### 2.2.1. Analysis of glycosyl composition and linkage

*Glycosyl composition analysis*: Glycosyl composition analysis was performed by combined gas chromatography/mass spectrometry (GC/MS) of the per-*O*-trimethylsilyl (TMS) derivatives of the monosaccharide methyl glycosides produced from the sample by acidic methanolysis. An aliquot was taken from the sample and added to separate tubes with 20 μg of Inositol as the internal standard. Methyl glycosides were then prepared from the dry sample following the mild acid treatment with 1 M HCl in methanol at 80 °C (16–18 h), followed by re-*N*-acetylation with pyridine and acetic anhydride in methanol (for detection of amino sugars). The sample was then per-*O*-trimethylsilylated by treatment with Tri-Sil (Pierce) at 80 °C (0.5 h). These procedures were carried out as previously described by Merkle and Poppe (1994) and York, Darvill, Mcneil, Stevenson, and Albersheim (1986). GC/MS analysis of the TMS methyl glycosides was performed on an AT 6890N GC interfaced to a 5975B MSD, using a Supelco EC-1 fused silica capillary column (30 m × 0.25 mm ID).

*Glycosyl linkage analysis*: The sample was permethylated, depolymerized, reduced, and acetylated; and the resultant partially methylated alditol acetates (PMAAs) analyzed by gas chromatography-mass spectrometry (GC-MS). Initially, one aliquot of each sample was suspended in about 200 μL of dimethyl sulfoxide. The sample was then permethylated by the method with treatment with sodium hydroxide and methyl iodide in dry DMSO. Following sample workup, the permethylated material was hydrolyzed using 2 M trifluoroacetic acid (2 h in sealed tube at

121 °C), reduced with $NaBD_4$, and acetylated using acetic anhydride/trifluoroacetic acid. The resulting PMAAs were analyzed on a Hewlett Packard 5890 GC interfaced to a 5970 MSD (mass selective detector, electron impact ionization mode); separation was performed on a 30 m Supelco 2330 bonded phase fused silica capillary column.

These two parts were finished commissioning Complex Carbohydrate Research Center in The University of Georgia.

#### 2.2.2. Solution preparation

SM-A87 EPS stock solution (9 g/L) was prepared by the dissolution of 9.0 g SM-A87 EPS in 1.0 L de-ionized water with stirring for more than 5 h at 25 °C. SM-A87 EPS solutions at low concentrations were obtained by the dilution of the stock solution with de-ionized water. The fresh solution was stored in the refrigerator at 4 °C and was used within three days, in order to avoid biodegradation. All of the solutions rested for at least 12 h before experiments.

#### 2.2.3. Rheological measurement

All of the rheological properties of SM-A87 EPS solution were measured by a controlled stress rheometer (RS75, Haake Inc., Germany) equipped with the Z41 concentric cylinder system at 30.0 ± 0.1 °C. Each sample rested for 10 min before the rheological measurement, in order to eliminate the effect of pouring and attain the temperature equilibrium.

*Creep and recovery measurement*: Creep and creep recovery tests were carried out as follows. At time $t = 0$, a constant shear stress ($\sigma$) was applied to the EPS solution and the compliance ($J$) was recorded as a function of $t$; at $t = 180$ s $\sigma$ was set to zero and the recoverable part of $J$ was measured as a function of the recovery time $t$. In order to make sure that $\sigma$ was in the linear viscoelastic region of SM-A87 EPS solutions with different concentrations ($C_{EPS}$), $\sigma$ was set to be 0.04 Pa at $C_{EPS} < 0.8$ g/L, 0.05 Pa at $C_{EPS} = 1.0$–2.0 g/L, 0.2 Pa at $C_{EPS} = 3.0$–5.0 g/L and 1.0 Pa at $C_{EPS} = 6.0$–9.0 g/L, respectively. In the low shear creep test, $\eta_0$ is the inverse of the slope of the compliance curve in the steady state flow regime, where the slope becomes constant according to Eq. (1) (Nicholls, 2006):

$$\frac{dJ}{dt} = \frac{1}{\eta_0} \tag{1}$$

*Flow curves*: For SM-A87 EPS solutions at various concentrations ($C_{EPS}$), the shear rate ($\dot{\gamma}$) was increased linearly from 0 to 1000 $s^{-1}$ in 5 min and then kept constant at 1000 $s^{-1}$ for 3 min. Then, the shear rate was decreased reversely from 1000 $s^{-1}$ to 0 in 5 min. During these three steps, the shear stress was measured correspondingly.

*Dynamic (Oscillatory) measurement*: For SM-A87 EPS solutions at various $C_{EPS}$, the stress sweep at the frequency $f = 0.5$ Hz was conducted from 0 to 50 Pa to determine the linear viscoelastic region. The angle frequency ($\omega = 2\pi f$) sweep was carried out at the stress of 0.05 Pa ($C_{EPS} > 0.8$ g/L) or 0.034 Pa ($C_{EPS} < 0.8$ g/L, accordingly) from 0.5 rad/s to 50 rad/s.

*Equilibrium viscosity*: Equilibrium viscosity ($\eta_{eq}$) is the apparent viscosity that does not change over time at some constant shear rate. $\eta_{eq}$ values at the shear rate of 1 $s^{-1}$, 10 $s^{-1}$, 100 $s^{-1}$, and 1000 $s^{-1}$ were measured at various concentrations of SM-A87 EPS solutions.

## 3. Results and discussion

### 3.1. Glycosyl composition and linkage analysis

The results of glycosyl composition and linkage analysis are listed in Table 1. From the monosaccharide unites it can be seen that the functional groups on a SM-A87 EPS molecule include hydroxyl, hemiacetal, aldehyde/ketone and carboxyl (Table 1) which were also verified by the FT-IR spectrum (Zhou et al., 2009). The existence of 3, 4-linked glucopyranosyl residue indicates that the SM-A87 EPS molecules are hyper-branched.

**Table 1**
Glycosyl composition analysis and glycosyl linkage analysis on raw sample.

| Glycosyl residue | mol% | Glycosyl residue | Percentage present |
|---|---|---|---|
| Fucose | 1.7 | Terminal mannopyranosyl residue | 1.2 |
| Xylose | 10.5 | 2-Linked mannopyranosyl residue | 17.3 |
| Glucuronic acid | 2.3 | 4-Linked mannopyranosyl residue | 17.1 |
| Mannose | 30.7 | Terminal glucopyranosyl residue | 15.4 |
| Galactose | 10.5 | 4-Linked glucopyranosyl residue | 1.7 |
| Glucose | 36.5 | 3,4-Linked glucopyranosyl residue | 12.3 |
| Unidentified sugar | 7.8 | 3-linked fucopyranosyl residue | 9.3 |
| | | Terminal galactopyranosyl residue | 16.3 |
| | | 3-Linked xylopyranosyl residue | 9.5 |

### 3.2. Critical concentrations

Critical concentrations, $C^*$ and $C^{**}$, are usually determined through the dependence of $\eta_0$ on the polymer or particle concentration (Benchabane & Bekkour, 2008; Biro et al., 2009; Candau, Regalado, & Selb, 1998; Ebagninin et al., 2009; Rodd et al., 2000). $\eta_0$ is measured mainly through the test of creep or oscillation (Nicholls, 2006). In this work, creep test was utilized to determine $\eta_0$ of SM-A87 EPS solutions. Fig. 1(A) shows the creep cures of SM-A87 EPS solutions in the $C_{EPS}$ range of 0.6–7.0 g/L. For clarity, all the collected data are not reported in the figure since they show similar trends (see Fig. S2 in supporting information). We found that $dJ/dt$ almost keeps constant in the last 30 s of creep test, and then $\eta_0$ values were determined as follows:

$$\eta_0 = \frac{30\ \text{s}}{J_{\text{end}} - J_{150}} \tag{2}$$

The dependence of $\eta_0$ of SM-A87 EPS solutions on $C_{EPS}$ is shown in Fig. 1(B). It can be seen that $\eta_0$ is positively associated with $C_{EPS}$ and the curve can be divided into three straight-line segments, corresponding to the dilute, semi-dilute and concentrated regimes (Adam et al., 1976). The concentrations at two crossover points can be determined as the overlapping concentration ($C^*$) and the crossover concentration ($C^{**}$). The $C^*$ and $C^{**}$ values of SM-A87 EPS solution obtained from Fig. 1(B) were 0.95 g/L and 4.99 g/L, respectively.

Usually, the critical concentrations can also be determined by the overlap parameter, $C{\cdot}[\eta]$, plotted as a function of the specific viscosity, $\eta_{sp}$, defined as (Clasen & Kulicke, 2001; Grigorescu & Kulicke, 2000):

$$\eta_{sp} = \frac{\eta_0 - \eta_s}{\eta_s} \tag{3}$$

and

$$[\eta] = \lim_{\substack{C_{EPS} \to 0 \\ \dot{\gamma} \to 0}} \left( \frac{\eta_{sp}}{C_{EPS}} \right) \tag{4}$$

where $C_{EPS}$ is SM-A87 EPS concentration; $[\eta]$, $\eta_s$ and $\eta_0$ are the intrinsic, the solvent and the zero shear rate viscosities, respectively.

$[\eta]$ of SM-A87 EPS solution was determined to be 0.84 L/g. Fig. 1(C) plots $\eta_{sp}$ as a function of the overlap parameter $C_{ESP}{\cdot}[\eta]$ for SM-A87 EPS solution. The slope changes at the values of $C_{ESP}{\cdot}[\eta] = 0.79$ and 4.20, which suggests the presence of two critical SM-A87 EPS concentrations, corresponding to the critical concentrations $C^* \sim 0.94$ g/L and $C^{**} \sim 5.00$ g/L. They are very close to the values obtained by creep tests (Fig. 1(B)). The $C^*{\cdot}[\eta]$ value of SM-A87 EPS solution is lower than those of the common polysaccharides such as carboxymethyl cellulose, high mannuronan alginate,

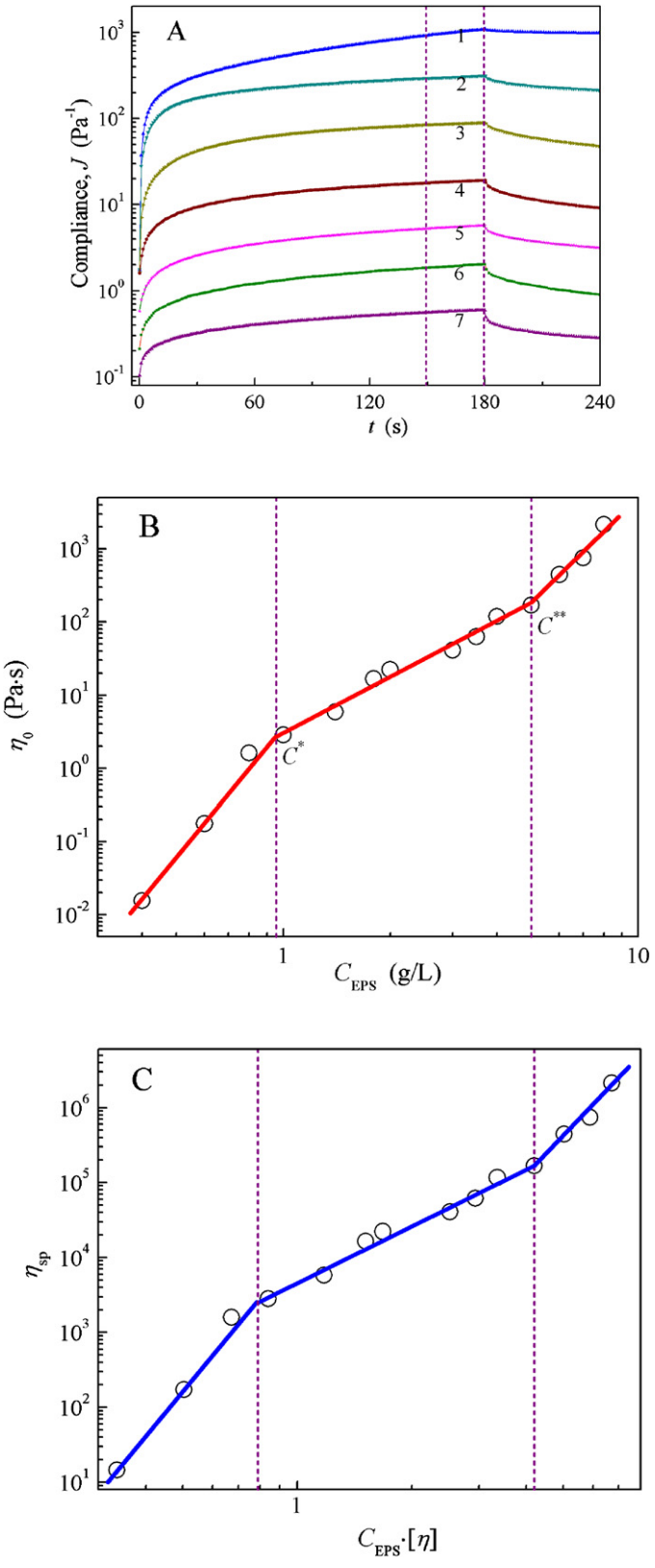


**Fig. 1.** (A) Creep curves of SM-A87 EPS solutions with various concentrations (g/L): (1) 0.6; (2) 0.8; (3) 1.4; (4) 2.0; (5) 3.5; (6) 5.0; (7) 7.0. (B) Zero-shear viscosity ($\eta_0$) of SM-A87 EPS solutions at different concentrations. (C) Specific viscosity ($\eta_{sp}$) as a function of the overlap parameter ($C_{EPS}\cdot[\eta]$). $C^*$ – overlapping concentration; $C^{**}$ – crossover concentration.

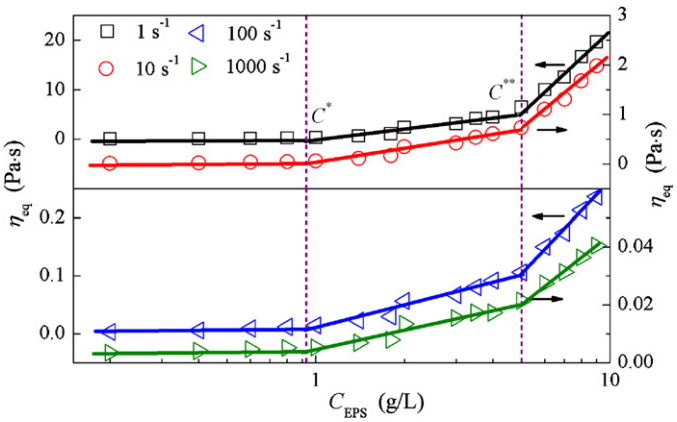


**Fig. 2.** The equilibrium viscosity ($\eta_{eq}$) of SM-A87 EPS solutions at different concentrations and shear rates.

λ-carragenan ($C^*[\eta]\approx 4$) (Morris, Cutler, Ross-Murphy, Rees, & Price, 1981), amilose ($C^*[\eta]=1$) (Ellis & Ring, 1985), dextran ($C^*[\eta]=0.8$–$2.2$) (Sabatié et al., 1988), guar-gum ($C^*[\eta]=1.0$) and locust bean gum ($C^*[\eta]=1.3$) (Doublier & Launay, 1981), but close to that of xanthan gum ($C^*[\eta]\approx 0.8$) (Gravanis, Milas, Rinaudo, & Tinland, 1987). The lower $C^*\cdot[\eta]$ value of SM-A87 EPS solution may be due to the stronger interaction among SM-A87 EPS molecules and the hyper-branched or stiff chains of SM-A87 EPS molecules. The interaction among SM-A87 EPS molecules may be induced mainly by H-bonding between the hydrogen on the hydroxyl and carboxyl and the oxygen on the aldehyde/ketone, carboxyl and hemiacetal groups since molecules of SM-A87 EPS are hyper-branched as revealed by three types of linkages (3, 4-linked glucopyranosyl residue) (see Table 1). This makes for the strong interactions among the SM-A87 EPS molecules, which results in $C^*$ of SM-A87 EPS solutions lower than that of the linear polysaccharide solutions (Doublier & Launay, 1981; Ellis & Ring, 1985; Morris et al., 1981; Sabatié et al., 1988). Izydorezyk and Biliaderis (1992) also considered that the $C^*[\eta]$ value of the solution of polysaccharide with stiff chains was lower than that of the linear polysaccharide solutions. The $C^*[\eta]$ value for the SM-A87 EPS solution is close to that of the xanthan gum solution because the xanthan gum molecules are also hyper-branched.

Fig. 2 shows the dependence of $\eta_{eq}$ of SM-A87 EPS solution at different shear rates on $C_{ESP}$. As can be seen, the slopes of curves change sharply twice as $C_{ESP}$ increases. The turning points correspond to the two critical concentrations, $C^*$ (0.93 g/L) and $C^{**}$ (5.01 g/L), respectively. These two critical values are nearly equal to the values determined through creep tests. In addition, the shear rate has no effect on the critical concentrations, as indicated in Fig. 2. Papanagopoulos et al. (1998) pointed out that in the case of linear polymer an increase of the shear rate provokes an increase of $C^*$, while in the case of highly branched polymer the shear rate has no influence on its critical concentration. The present results of the shear rate-independence of $C^*$ indicates that the studied SM-A87 EPS molecules should be hyper-branched, which is in accordance with the result of glycosyl linkage analysis (Table 1). Besides, it can be concluded that as for the hyper-branched polymer solution, $C^*$ and $C^{**}$ may be determined through the dependence of the equilibrium viscosity at some shear rate on the solution concentration.

### 3.3. Thixotropy

Fig. 3(A) shows the hysteresis loops of SM-A87 EPS solutions at various $C_{ESP}$. For clarity, all the collected data are not reported in the figure since they show similar trends (see Fig. S3

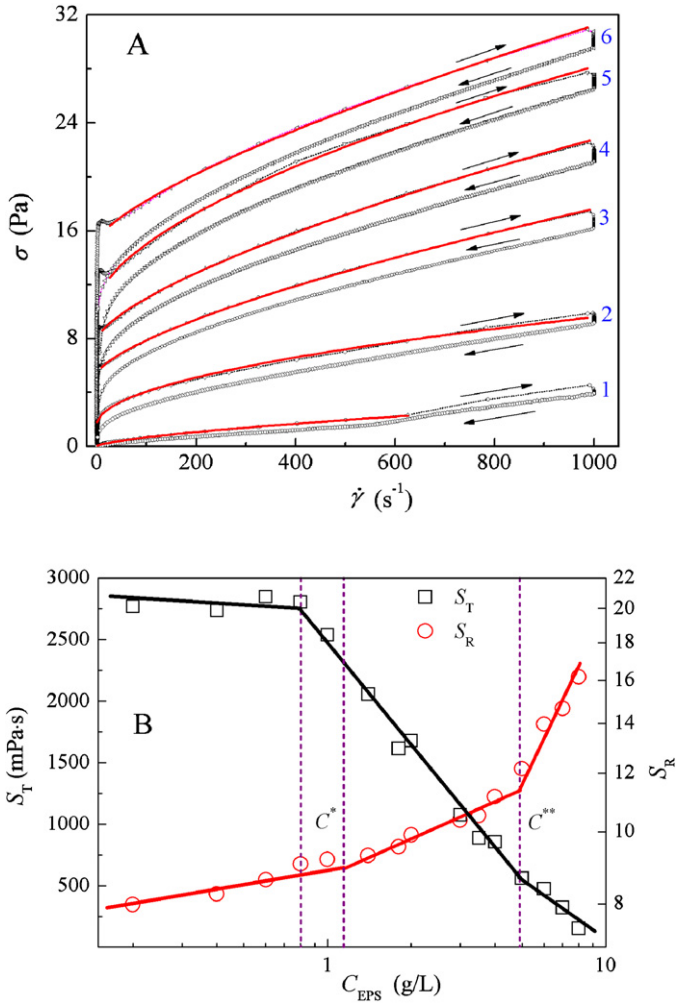


**Fig. 3.** (A) Hysteresis loops of SM-A87 EPS solutions at different concentrations (g/L): (1) 0.4; (2) 2.0; (3) 4.0; (4) 5.0; (5) 6.0; (6) 7.0. (B) Absolute ($S_T$) and relative ($S_R$) thixotropic strength of SM-A87 EPS solutions at different concentrations ($C_{EPS}$).

in supporting information). It can be seen that all the up curves of hysteresis loops are above the down curves, indicating that all the SM-A87 EPS solutions in the studied $C_{ESP}$ range of 0.2–8.0 g/L display positive thixotropy. For the SM-A87 EPS solution with $C_{EPS}$ higher than $C^*$, the appearance of positive thixotropy is not a surprise, which may be attributed to the three-dimensional networks existing in the solution (see Fig. S4 in supporting information). The formation of three-dimensional networks may be due to H-bonding among the SM-A87 EPS molecules. At higher shear rate the network structures existing in the solution may be gradually destroyed by shearing and then at lower shear rate, the destroyed structures may be recovered, but the structure recovery process has a relaxation time, which results in thixotropy exhibited by the solutions. However, the positive thixotropy of SM-A87 EPS solution with $C_{EPS}$ less than $C^*$ may arise from the shear-induced molecular orientation on the shearing direction.

The area of hysteresis loop ($S_T$), *i.e.*, the area enclosed by up curve and down curve, may be thought to be an estimation of the strength of thixotropy. Generally speaking, greater hysteresis area means stronger thixotropy (Cheng & Evans, 1965; Dolz, González, Delegido, Hernández, & Pellicer, 2000; Mewis, 1979). In addition, the relative thixotropic area, $S_R$, was also proposed to reflect the thixotropic strength (Dolz, Hernández, Pellicer, & Delegido, 1995; Dolz, Hernández, Delegido, Alfaro, & Muñoz, 2007):

$$S_R(\%) = 100 \times \frac{S_T}{S_D} \quad (5)$$

where $S_D$ is the area enclosed by the up curve and *X*-axis. The $S_T$ and $S_R$ may be used to represent absolute and relative thixotropic strength, respectively. Fig. 3(B) shows the changes of the absolute thixotropic strength ($S_T$) and the relative thixotropic strength ($S_R$) with the solution concentration. It can be seen that the absolute thixotropic strength increases while the relative thixotropic strength decreases with the $C_{EPS}$ increasing. Dolz et al. (1995) also found the different dependence of absolute and relative thixotropic strength on the concentration in the complex system of microcrystalline cellulose-sodium carboxymethyl cellulose and starch. With the $C_{EPS}$ increasing, the increase of the absolute thixotropic strength arises from the strengthening of the three-dimensional networks, while the decrease of the relative thixotropic strength may arise from the speeded-up of the recovery velocity of the destroyed structures.

The curves of thixotropic strength *vs.* $C_{EPS}$ in Fig. 3(B) exhibit two abrupt slope changes. The changes correspond to $C^*$ and $C^{**}$ values of 0.80–1.14 g/L and 4.91 g/L, respectively, which are nearly equal to the values determined through creep tests (Fig. 1(B)). So, we conclude that for the thixotropic solution, the measurement of thixotropic strength can be used for the determination of $C^*$ and $C^{**}$.

### 3.4. Flow curves

For SM-A87 EPS solutions at various concentrations, the flow curves, *i.e.*, the up curves of hysteresis loops (Fig. 3(A)), display the existence of static yield stress with $C_{EPS}$ more than 1 g/L and no static yield stress with $C_{EPS}$ less than 1 g/L. The dynamic yield stresses were obtained by fitting the flow curves of hysteresis loops (solid lines in Fig. 3(A)) with Herschel–Bulkley model:

$$\sigma = \sigma_0 + k \cdot \dot{\gamma}^n \quad (6)$$

where $\sigma$ is the shear stress (Pa), $\dot{\gamma}$ the shear rate (s$^{-1}$), $k$ the consistency coefficient (Pa s$^n$), $\sigma_0$ the dynamic yield stress (Pa) and $n$ the fluidity index (dimensionless). Fig. 4(A) shows the static yield stress and the dynamic yield stresses obtained from the up curves and the down curves of hysteresis loops, respectively. All the curves exhibit abrupt slope changes with $C_{EPS}$ increasing, corresponding to $C^*$ and $C^{**}$ values of 1.00 g/L and 4.96 g/L, respectively. Both values are almost equal to the values determined by creep tests. Other parameters, $k$ and $n$, of Herschel–Bulkley model for flow curves are shown in Fig. 4(B). The increase of $k$ and the decrease of $n$ with the solution concentration increasing indicate the increase of solution viscosity and strengthening deviation from Newtonian fluid, respectively. Obviously, the curves of $k$ or $n$ *vs.* $C_{EPS}$ display three parts and the overcross points should correspond to $C^*$ and $C^{**}$. $C^*$ and $C^{**}$ may be obtained from Fig. 4(B) to be 0.80–1.06 g/L and 4.73–5.00 g/L, respectively.

In addition, it can be seen from Fig. 4(A) that the dynamic yield stresses obtained from the up curves are more than those from the down curves. Both the dynamic yield stresses are less than the static yield stresses, which is consistent with the current results (Banchathanakij & Suphantharika, 2009; Cheng, 1986; Yang et al., 2009). The coexistence of static and dynamic yield stresses of the SM-A87 EPS solutions may be explained following Cheng's point of view (Cheng, 1986), *i.e.*, there may be more than one type of structures in a thixotropic fluid. Here, two types of structures may be considered. One is the steric and electric repulsion among hydrated SM-A87 EPS molecules (the contact of hydrated lays of SM-A87 EPS molecules rather than the molecules themselves) which is not sensitive to shear rate. So, some stress is always needed to

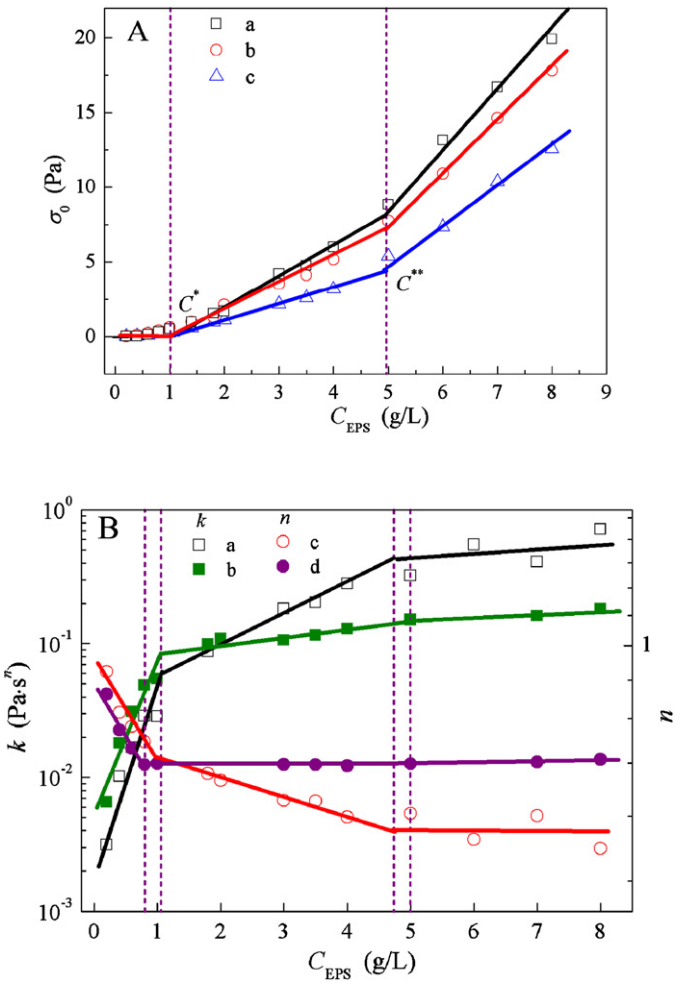


**Fig. 4.** (A) Yield stress ($\sigma_0$) of SM-A87 solutions at different concentrations: (a) static yield stress; (b) dynamic yield stress from up curves of hysteresis loops; (c) dynamic yield stress from down curves of hysteresis loops. (B) Consistency coefficient, $k$ and fluidity index, $n$ from Herschel-Bulkley model for up (b and d) and down curves (a and c) of hysteresis loop of SM-A87 EPS solutions at different concentrations.

keep the solutions flowing from the point at which the dynamic yield stress is displayed. However, when the density of hydrated molecules, *i.e.*, the solution concentration, increases and exceeds a critical value ($C^*$), the second type of structures, three-dimensional networks, will be formed due to the hydrogen bonding among SM-A87 EPS molecules when solutions rested, and a stress is needed to make the solution flow. This stress is just the static yield stress. When the solution concentration is less than 1.0 g/L, the density of hydrated molecules is so small that no three-dimensional networks are formed, which causes the static yield stress to overlap with the dynamic yield stress. When the solution concentration is greater than 1.0 g/L, the three-dimensional networks start to form and the static yield stress is greater than the dynamic stress (Fig. 4(A) a and b). That the dynamic yield stress obtained from up curves is greater than that from down curves (Fig. 4(A) b and c) may be due to the positive thixotropy of the solution.

### 3.5. Critical shear rate

Fig. 5 shows the viscosity of SM-A87 EPS solutions as a function of shear rate at different concentrations (corresponding to the up curves of hysteresis loops in Fig. 3(A)). All of the solutions in the studied $C_{ESP}$ range of 0.4–8.0 g/L exhibit an initial shear-thickening behavior, where the apparent viscosity increases with increasing

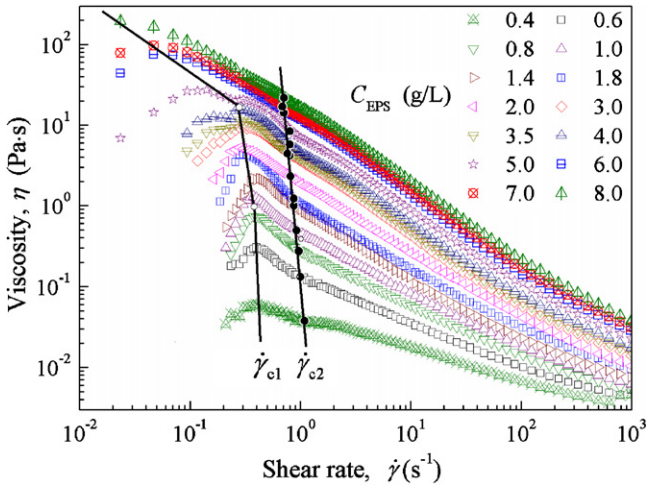


**Fig. 5.** Viscosity ($\eta$) as a function of shear rate ($\dot{\gamma}$) of SM-A87 EPS solutions at different concentrations.

shear rate to reach a maximum value, followed by a shear-thinning behavior at a given shear rate (named as first critical shear rate, $\dot{\gamma}_{c1}$). The shear-thinning region may be subdivided into two parts by the second critical shear rate ($\dot{\gamma}_{c2}$) at which the decreasing rate of the viscosity with increasing shear rate changes. Similar results were observed in poly(ethylene oxide) (Ebagninin et al., 2009) and carboxymethyl cellulose (Benchabane & Bekkour, 2008) solutions. Few researches on this peculiar shear-thickening behavior at low shear rate in polymer solutions have been reported. The mechanism for the behavior is still elusive. Various explanations have been proposed to explain the shear thickening behavior of polymer solutions. One of the most accepted interpretations is the "flow-induced formation of macromolecular associations" proposed by Liu, Yu, and Lin (2007). Ebagninin et al. (2009) and Benchabane and Bekkour (2008) agreed with what Liu et al. (2007) proposed and believed that the shear thickening behavior of poly(ethylene oxide) (Ebagninin et al., 2009) and carboxymethyl cellulose (Benchabane & Bekkour, 2008) solutions were the determinants of the formation of a stiffer inner structure due to the entanglements of polymer coils and the increase in the intermolecular interactions as the shear rate rose. We adopt the mechanism proposed by Liu et al. (2007) to interpret the shear-thickening behavior of SM-A87 EPS solutions at low shear rate and argue that the increase in the intermolecular interaction should be principal. For the shear-thinning behavior at higher shear rate, a well-accepted mechanism is due to the increased orientation of the polymer coils in the direction of the flow and the disentanglement among the polymer coils in solution (Clasen & Kulicke, 2001; Dunstan, Hill, & Wei, 2004). This can be used to explain the shear-thinning behavior of SM-A87 EPS solutions at higher shear rate. The first shear-thinning stage ($\dot{\gamma}_{c1} < \dot{\gamma} < \dot{\gamma}_{c2}$) may have arisen mainly from the orientation of the polymer coils in the direction of the flow, and the second shear-thinning stage ($\dot{\gamma} > \dot{\gamma}_{c2}$) may have arisen mainly from the disentanglement among the polymer coils in solution.

Fig. 6(A) shows the changes of $\dot{\gamma}_{c1}$ and the viscosity ($\eta_{c1}$) at $\dot{\gamma}_{c1}$ with $C_{EPS}$. With increasing $C_{EPS}$, $\dot{\gamma}_{c1}$ decreases gradually while $\eta_{c1}$ increases gradually. Both of the curves display two turning points as $C_{EPS}$ closes to $C^*$ and $C^{**}$. The decrease of $\dot{\gamma}_{c1}$ with $C_{EPS}$ indicates that the effect of the polymer coil orientation in the flow direction on the viscosity of the solution is strengthened at higher $C_{EPS}$. The changing tendency of $\eta_{c1}$ with $C_{EPS}$ is similar to that of $\eta_0$ with $C_{EPS}$. Fig. 6(B) shows the dependence of $\eta_{c1}$ on $\dot{\gamma}_{c1}$, there is a turning point to divide the curve into two parts, both of which fit well with the

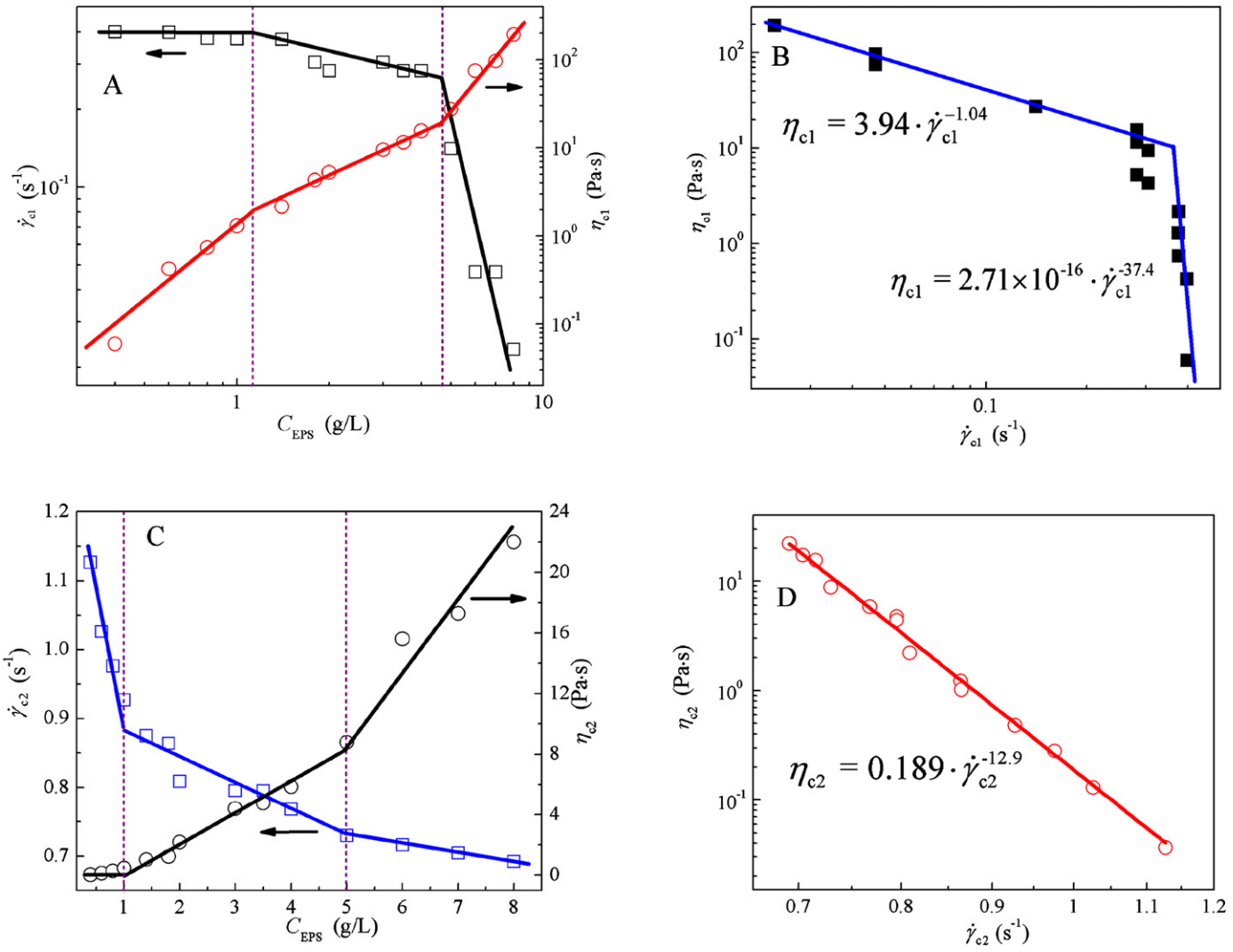


**Fig. 6.** (A) The first critical shear rate ($\dot{\gamma}_{c1}$) and the viscosity ($\eta_{c1}$) at $\dot{\gamma}_{c1}$ as a function of the SM-A87 EPS concentration. (B) The dependence of $\eta_{c1}$ on $\dot{\gamma}_{c1}$. (C) The second critical shear rate ($\dot{\gamma}_{c2}$) and the viscosity ($\eta_{c2}$) at $\dot{\gamma}_{c2}$ as a function of the SM-A87 EPS concentration. (D) The dependence of $\eta_{c2}$ on $\dot{\gamma}_{c2}$.

power law model:

$$\eta_{c1} = (3.94 \pm 0.43) \cdot \dot{\gamma}_{c1}^{(-1.04\pm0.03)} \quad (7)$$

$$\eta_{c1} = (2.71 \pm 0.80) \times 10^{-16} \cdot \dot{\gamma}_{c1}^{(-37.4\pm3.0)} \quad (8)$$

with the adjusted relative coefficient to be 0.999 and 0.954, respectively.

Fig. 6(C) shows the changes of $\dot{\gamma}_{c2}$ and the viscosity ($\eta_{c2}$) at $\dot{\gamma}_{c2}$ with $C_{EPS}$, it can be seen that with increasing $C_{EPS}$, $\dot{\gamma}_{c2}$ decreases while $\eta_{c2}$ increases. Both of the curves also display two turning points at $C_{EPS}$ close to $C^*$ and $C^{**}$. The decrease of $\dot{\gamma}_{c2}$ with $C_{EPS}$ indicates that the effect of the disentanglement among the polymer coils on the viscosity of the solution is strengthened at higher $C_{EPS}$. The plot of $\eta_{c2}$ *vs.* $\dot{\gamma}_{c2}$ is shown in Fig. 6(D), and a power law equation may be obtained as:

$$\eta_{c2} = (0.189 \pm 0.052) \cdot \dot{\gamma}_{c2}^{(-12.9\pm0.8)} \quad (9)$$

with the adjusted relative coefficient to be 0.985. Similar result was reported for carboxymethyl cellulose solution (Benchabane & Bekkour, 2008).

### 3.6. Storage and loss modulus

Fig. 7(A) shows the storage modulus ($G'$) and loss modulus ($G''$) as a function of angular frequency ($\omega$) at the stress of 0.05 Pa (in the linear viscoelastic region). For clarity, all the collected data are not reported in the figure since they show similar trend. Both $G'$ and $G''$ increase with the angular frequency and solution concentration. The solutions with $C_{EPS}$ less than 1.0 g/L exhibit $G''$ higher than $G'$ in the studied $\omega$ range, indicating that the viscous properties are dominant compared to the elastic ones. At $C_{EPS}$ in the range of 1.0–1.8 g/L, a transition can be observed at the higher angular frequency, where $G'$ are found to be higher than $G''$, indicating that the viscoelastic properties appear. After $C_{EPS}$ more than 2.0 g/L, $G'$ is higher than $G''$ in the studied $\omega$ range, indicating the elastic properties are dominant compared to the viscous ones. The appearance of viscoelastic behavior could be related to the formation of a three-dimensional network, indicating the solutions transform from liquid-like fluid to solid-like fluid. It can be seen from Fig. 7(A) that the angular frequency ($\omega^*$) at the intersection of $G'$ and $G''$ decreases with $C_{EPS}$. Therefore, the characteristic time ($2\pi/\omega^*$), related to the longest relaxation time and to the information about the lifetime of associative network (Chronakis & Alexandridis, 2001), will increase, *i.e.*, the lifetime of the network will be prolonged with $C_{EPS}$.

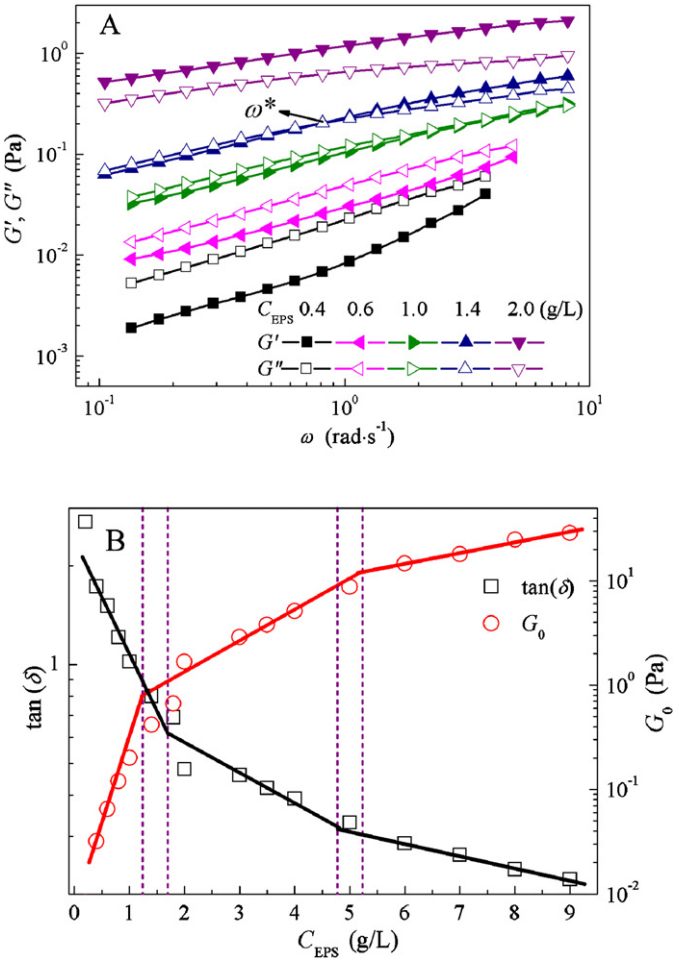


**Fig. 7.** (A) Dependence of storage modulus ($G'$) and loss modulus ($G''$) on the angular frequency ($\omega$) at the stress of 0.05 Pa. (B) Dependence of phase angle tangent ($\tan(\delta)$) and storage modulus ($G_0$) in the linear viscoelastic region on the SM-A87 EPS concentrations at the frequency of 0.5 Hz.

Fig. 7(B) shows the dependence of phase angle tangent ($\tan(\delta)$) and elastic modulus ($G_0$) at the frequency of 0.5 Hz in the linear viscoelastic region on $C_{EPS}$. The slope changes of both of the curves at the critical concentrations $C^*$ (1.24–1.69 g/L) and $C^{**}$ (4.78–5.23 g/L) took place. Similar results were observed in *Aeromonas* gum solutions (Xu, Liu, & Zhang, 2006) and cellulous solutions (Lue & Zhang, 2009). The $\tan(\delta)$ value more than 1 means a dominant viscous behavior, while the $\tan(\delta)$ value less than 1 means a dominant elastic behavior. It can be concluded from results of Fig. 7(B) that the overlapping concentration, $C^*$, could be considered as the critical concentration at which the viscoelastic properties do appear in the polymer solutions. But it is also reported that crossover concentration, $C^{**}$, could be considered as the critical concentration at which the viscoelastic properties do appear in poly(ethylene oxide) (Ebagninin et al., 2009) and carboxymethyl cellulose (Benchabane & Bekkour, 2008) solutions. The hyper-branched molecular structure and strong inter-molecular H-bonding of SM-A87 EPS may be the reason that the SM-A87 EPS solution can display dominant elastic behavior at lower concentration. This is favorable for its application in enhanced oil recovery system.

## 4. Conclusion

The rheological properties, such as shear flow behavior, thixotropy and viscoelasticity, of the solution of a new type of exopolysaccharide (SM-A87 EPS) secreted by deep-sea mesophilic bacterium were investigated. Zero-shear viscosities of the solutions at different concentrations were determined using creep tests. The concentration-dependence of zero-shear viscosity showed the existence of two critical concentrations, *i.e.*, overlapping concentration $C^*$ and crossover concentration $C^{**}$, to be 0.95 g/L and 4.99 g/L, respectively, which were confirmed by the concentration-dependences of other rheological parameters, such as equilibrium viscosity, thixotropic strength, static and dynamic stress, critical shear rate, and storage modulus in the linear viscoelastic region of the SM-A87 EPS solutions. At concentrations higher than $C^*$, the solutions exhibited a static stress, a dominant elastic behavior, a stronger absolute positive thixotropic strength; otherwise, at concentrations lower than $C^*$, no static stress, a dominant viscous behavior and a weaker absolute positive thixotropic strength were exhibited. At above a critical shear rate ($\dot{\gamma}_{c1}$), all SM-A87 EPS solutions in the studied concentration (0.4–8.0 g/L) exhibited a shear-thinning behavior, and there was a critical shear rate ($\dot{\gamma}_{c2}$) at which the decreasing rate of the viscosity with the shear rate increasing changed obviously. The SM-A87 EPS solutions may be used as enhanced oil recovery system.

## Acknowledgements

This work was supported by the National Natural Science Foundation of China (No. 50772062), the Natural Science Foundation of Shandong Province of China (No. Z2008B08) and Taishan Scholar Foundation of Shandong Province of China (No. ts20070713).

## Appendix A. Supplementary data

Supplementary data associated with this article can be found, in the online version, at doi:10.1016/j.carbpol.2010.12.072.

## References

Abu-Jdayil, B., Al-Malah, K., & Asoud, H. (2002). Rheological characterization of milled sesame (tehineh). *Food Hydrocolloids*, *16*, 55–61.
Adam, M., Delsanti, M., & Jannink, G. (1976). Light scattering by cooperative diffusion in semi-dilute polymer solutions. *Journal of Physique Letter*, *37*, 53–56.
Banchathanakij, R., & Suphantharika, M. (2009). Effect of different beta-glucans on the gelatinisation and retrogradation of rice starch. *Food Chemistry*, *114*, 5–14.
Barnes, H. A. (1999). The yield stress–a review or 'παντα ροι'-everything flows? *Journal of Non-Newtonian Fluid Mechanics*, *81*, 133–178.
Barnes, H. A., & Walters, K. (1985). The yield stress myth? *Rheologica Acta*, *24*, 323–326.
Benchabane, A., & Bekkour, K. (2008). Rheological properties of carboxymethyl cellulose (CMC) solutions. *Colloid and Polymer Science*, *286*, 1173–1180.
Biro, S., Gandhi, T., & Amirkhanian, S. (2009). Determination of zero shear viscosity of warm asphalt binders. *Construction and Building Materials*, *23*, 2080–2086.
Blair, G. W. S. (1933). On the nature of "yield-value". *Physics*, *4*, 113–118.
Bradna, P., & Quadrat, O. (1984). Criteria of negative thixotropy of poly(methyl methacrylate) solutions as a function of temperature and of the thermodynamic quality and viscosity of the solvent. *Colloid and Polymer Science*, *262*, 189–196.
Bradna, P., Quadrat, O., & Dupuis, D. (1995). Negative thixotropy of solutions of partially hydrolyzed polyacrylamide. *Colloid and Polymer Science*, *273*, 642–647.
Candau, F., Regalado, E. J., & Selb, J. (1998). Scaling behavior of the zero shear viscosity of hydrophobically modified poly(acrylamide)s. *Macromolecules*, *31*, 5550–5552.
Cheng, D. C. H. (1986). Yield stress: A time-dependent property and how to measure it. *Rheologica Acta*, *25*, 542–554.
Cheng, D. C. H., & Evans, F. (1965). Phenomenological characterization of the rheological behaviour of inelastic reversible thixotropic and antithixotropic fluids. *British Journal of Applied Physics*, *16*, 1599–1617.
Choi, S., & Han, C. D. (2003). Molecular weight dependence of zero-shear viscosity of block copolymers in the disordered state. *Macromolecules*, *37*, 215–225.
Chronakis, I. S., & Alexandridis, P. (2001). Rheological properties of oppositely charged polyelectrolyte–surfactant mixtures: Effect of polymer molecular weight and surfactant architecture. *Macromolecules*, *34*, 5005–5018.
Clasen, C., & Kulicke, W. M. (2001). Determination of viscoelastic and rheo-optical material functions of water-soluble cellulose derivatives. *Progress in Polymer Science*, *26*, 1839–1919.
Dai, X. N., Hou, W. G., Duan, H. D., & Ni, P. (2007). Thixotropy of Mg-Al-layered double hydroxides/kaolinite dispersion. *Colloids and Surfaces A: Physicochemical and Engineering Aspects*, *295*, 139–145.

Dolz, M., Bbugaj, J., Pellicer, J., Hernández, M. J., & Górecki, M. (1997). Thixotropy of highly viscous sodium (carboxymethyl)cellulose hydrogels. *Journal of Pharmaceutical Sciences*, *86*, 1283–1287.

Dolz, M., González, F., Delegido, J., Hernández, M. J., & Pellicer, J. (2000). A time-dependent expression for thixotropic areas. Application to Aerosil 200 hydrogels. *Journal of Pharmaceutical Sciences*, *89*, 790–797.

Dolz, M., Hernández, M. J., Delegido, J., Alfaro, M. C., & Muñoz, J. (2007). Influence of xanthan gum and locust bean gum upon flow and thixotropic behaviour of food emulsions containing modified starch. *Journal of Food Engineering*, *81*, 179–186.

Dolz, M., Hernández, M. J., Pellicer, J., & Delegido, J. (1995). Shear stress synergism index and relative thixotropic area. *Journal of Pharmaceutical Sciences*, *84*, 728–732.

Doublier, J. L., & Launay, B. (1981). Rheology of galactomannan solutions-comparative study of gum and locust bean gum. *Journal of Texture Studies*, *12*, 151–172.

Dunstan, D. E., Hill, E. K., & Wei, Y. (2004). Direct measurement of polymer segment orientation and distortion in shear: Semi-dilute solution behavior. *Polymer*, *45*, 1261–1266.

Ebagninin, K. W., Benchabane, A., & Bekkour, K. (2009). Rheological characterization of poly(ethylene oxide) solutions of different molecular weights. *Journal of Colloid and Interface Science*, *336*, 360–367.

Ellis, H. S., & Ring, S. G. (1985). A study of some factors influencing amylose gelation. *Carbohydrate Polymers*, *5*, 201–213.

Gravanis, G., Milas, M., Rinaudo, M., & Tinland, B. (1987). Comparative behavior of the bacterial polysaccharides xanthan and succinoglycan. *Carbohydrate Research*, *160*, 259–265.

Grigorescu, G., & Kulicke, W. M. (2000). *Prediction of viscoelastic properties and shear stability of polymers in solution viscoelasticity, atomistic models, statistical chemistry* Berlin/Heidelberg: Springer., pp. 1–40

Hou, W. G., Sun, D. J., Han, S. H., Zhang, C. G., & Wang, G. T. (1998). Study on the thixotropy of aluminum magnesium hydroxide– Na-montmorillonite suspension. *Colloid and Polymer Science*, *276*, 274–277.

Li, S. P., Hou, W. G., Sun, D. J., Guo, P. Z., Jia, C. X., & Hu, J. F. (2003). The thixotropic properties of hydrotalcite-like/montmorillonite suspensions. *Langmuir*, *19*, 3172–3177.

Liu, W. H., Yu, T. L., & Lin, H. L. (2007). Shear thickening behavior of dilute poly(diallyl dimethyl ammonium chloride) aqueous solutions. *Polymer*, *48*, 4152–4165.

Lue, A., & Zhang, L. (2009). Rheological behaviors in the regimes from dilute to concentrated in cellulose solutions dissolved at low temperature. *Macromolecular Bioscience*, *9*, 488–496.

Lund, R., Lauten, R. A., Nyström, B., & Lindman, B. (2001). Linear and nonlinear viscoelasticity of semidilute aqueous mixtures of a nonionic cellulose derivative and ionic surfactants. *Langmuir*, *17*, 8001–8009.

Izydorczyk, M. S., & Biliaderis, C. G. (1992). Influence of structure on the physicochemical properties of wheat arabinoxylan. *Carbohydrate Polymers*, *17*, 237–247.

Merkle, R. K., & Poppe, I. (1994). Carbohydrate composition analysis of glycoconjugates by gas-liquid chromatography/mass spectrometry. *Methods in Enzymology*, *230*, 1–15.

Mewis, J. (1979). Thixotropy—a general review. *Journal of Non-Newtonian Fluid Mechanics*, *6*, 1–20.

Moller, P. C. F., Mewis, J., & Bonn, D. (2006). Yield stress and thixotropy: On the difficulty of measuring yield stresses in practice. *Soft Matter*, *2*, 274–283.

Morris, E. R., Cutler, A. N., Ross-Murphy, S. B., Rees, D. A., & Price, J. (1981). Concentration and shear rate dependence of viscosity in random coil polysaccharide solutions. *Carbohydrate Polymers*, *1*, 5–21.

Nicholls, C. (2006). Analysis of available data on validation of bitumen tests. *Report on phase I of the BiTVal project, Forum of European National Highway Research Laboratories*. http://bitval.fehrl.org/fileadmin/bitval/BitVal_final_report.pdf.

Papanagopoulos, D., Pierri, E., & Dondos, A. (1998). Influence of the shear rate, of the molecular architecture and of the molecular mass on the critical overlapping concentration $C^*$. *Polymer*, *39*, 2195–2199.

Qin, Q. L., Zhao, D. L., Wang, J., Chen, X. L., Dang, H. Y., Li, T. G., et al. (2007). Wangia profunda gen. nov., sp. nov., a novel marine bacterium of the family Flavobacteriaceae isolated from southern Okinawa Trough deep-sea sediment. *FEMS Microbiology Letters*, *271*, 53–58.

Quadrat, O. (1985). Negative thixotropy in polymer solutions. *Advances in Colloid and Interface Science*, *24*, 45–75.

Rodd, A. B., Dunstan, D. E., & Boger, D. V. (2000). Characterisation of xanthan gum solutions using dynamic light scattering and rheology. *Carbohydrate Polymers*, *42*, 159–174.

Roots, J., & Nyström, B. (1979). Transition between dilute and concentrated solution behaviour as revealed by excimer fluorescence. *European Polymer Journal*, *15*, 1127–1131.

Sabatié, J., Choplin, L., Doublier, J. L., Arul, J., Paul, F., & Monsan, P. (1988). Rheology of native dextrans in relation to their primary structure. *Carbohydrate Polymers*, *9*, 287–299.

Stadler, F., Piel, C., Kaschta, J., Rulhoff, S., Kaminsky, W., & Münstedt, H. (2006). Dependence of the zero shear-rate viscosity and the viscosity function of linear high-density polyethylenes on the mass-average molar mass and polydispersity. *Rheologica Acta*, *45*, 755–764.

Takigawa, T., Kadoya, H., Miki, T., Yamamoto, T., & Masuda, T. (2006). Dependence of zero-shear viscosity and steady-state compliance on molecular weight between entanglements for ethylene-cycloolefin copolymers. *Polymer*, *47*, 4811–4815.

Xu, X. J., Liu, W. H., & Zhang, L. N. (2006). Rheological behavior of Aeromonas gum in aqueous solutions. *Food Hydrocolloids*, *20*, 723–729.

Yang, F., Bick, A., Shandalov, S., Brenner, A., & Oron, G. (2009). Yield stress and rheological characteristics of activated sludge in an airlift membrane bioreactor. *Journal of Membrane Science*, *334*, 83–90.

Ying, Q. C., & Chu, B. (1987). Overlap concentration of macromolecules in solution. *Macromolecules*, *20*, 362–366.

York, W. S., Darvill, A. G., Mcneil, M., Stevenson, T. T., & Albersheim, P. (1986). Isoloaton and characterization of plant-cell walls and cell-wall components. *Methods in Enzymology*, *118*, 3–40.

Zhou, W. Z., Wang, J., Shen, B. L., Hou, W. G., & Zhang, Y. Z. (2009). Biosorption of copper(II) and cadmium(II) by a novel exopolysaccharide secreted from deep-sea mesophilic bacterium. *Colloids and Surfaces B: Biointerfaces*, *72*, 295–302.